Jaka Čemažar
Tadej Kotnik

Faculty of Electrical Engineering, University of Ljubljana, Ljubljana, Slovenia

Received March 15, 2012
Revised June 21, 2012
Accepted June 27, 2012

Research Article

Dielectrophoretic field-flow fractionation of electroporated cells

We describe the development and testing of a setup that allows for DEP field-flow fractionation (DEP-FFF) of irreversibly electroporated, reversibly electroporated, and nonelectroporated cells based on their different polarizabilities. We first optimized the channel and electrode dimensions, flow rate, and electric field parameters for efficient DEP-FFF separation of moderately heat-treated CHO cells (50°C for 15 min) from untreated ones, with the former used as a uniform and stable model of electroporated cells. We then used CHO cells exposed to electric field pulses with amplitudes from 1200 to 2800 V/cm, yielding six groups containing various fractions of nonporated, reversibly porated, and irreversibly porated cells, testing their fractionation in the chamber. DEP-FFF at 65 kHz resulted in distinctive flow rates for nonporated and each of the porated cell groups. At lower frequencies, the efficiency of fractionation deteriorated, while at higher frequencies the separation of individual elution profiles was further improved, but at the cost of cell flow rate slowdown in all the cell groups, implying undesired transition from negative into positive DEP, where the cells are pulled toward the electrodes. Our results demonstrate that fractionation of irreversibly electroporated, reversibly electroporated, and nonelectroporated cells is feasible at a properly selected frequency.

Keywords:
Cell fractionation / Dielectrophoresis / Electroporation / Microfluidics
DOI 10.1002/elps.201200265

1 Introduction

An exposure of a cell to a sufficiently high external electric field results in electroporation–formation of nanoscale aqueous pores in the lipid bilayer of the cell plasma membrane [1–3]. These permeable structures provide a pathway for diffusive inflow of otherwise membrane-impermeant exogenous molecules into the cells, as well as outflow of biomolecules from the cells. If the exposure is sufficiently short and the membrane recovers sufficiently rapidly for the cell to remain viable, electroporation is reversible, otherwise it is irreversible. Reversible electroporation is already an established method for introduction of membrane-impermeant chemotherapeutics into tumor cells–electrochemotherapy [4], and a promising technique for gene therapy devoid of the risks caused by viral vectors–gene electrotransfer [5]. In medicine, irreversible electroporation is a method for tissue ablation–nonthermal electroablation [6], while in biotechnology it is used in electroextraction of biomolecules [7] and microbial deactivation, particularly in food preservation [8].

For optimal efficiency of a particular application of electroporation, all the exposed cells should be electroporated as uniformly as possible. In electrochemotherapy and gene electrotransfer, electroporation of all the cells should thus be reversible, while in electroablation, electroextraction, and microbial deactivation, it should be irreversible. In practice, however, such an ideal is difficult to achieve, as the cells can vary in their size, shape, phase of the cell cycle, orientation, membrane composition, etc. As a result, if the applied electric field pulses are relatively weak and/or short, one avoids irreversible electroporation, but some cells are not porated at all, while with stronger and/or longer pulses, all the cells are porated, but unavoidably some of them are porated irreversibly [9]. Furthermore, even if the goal is to achieve irreversible poration of all the exposed cells, a pulse amplitude required for this is often either technologically unachievable, or results in substantial heating that can be detrimental to the patient (in electroablation, which should be nonthermal) or the composition of the sample (in electroextraction and food preservation). In general, in every application of electroporation, the electric field applied is thus an empirically determined compromise that yields as many cells as possible

Correspondence: Dr. Tadej Kotnik, Faculty of Electrical Engineering, University of Ljubljana, Tržaška 25, SI-1000 Ljubljana, Slovenia
E-mail: tadej.kotnik@fe.uni-lj.si
Fax: +38-614-26-4658

Abbreviations: DEP-FFF, DEP field-flow fractionation; **MTS**, methyl-tetrazolium salt (3-(4,5-dimethylthiazol-2-yl)-5-(3-carboxymethoxyphenyl)-2-(4-sulfophenyl)-2H-tetrazolium); **PI**, propidium iodide

Colour Online: See the article online to view Figs. 2 and 4 in colour.

porated in the preferred manner, with small fractions of cells porated differently or not at all.

In fundamental research of electroporation in vitro, particularly in investigating the intracellular effects of reversible or/and irreversible poration, it would be useful to perform the studies separately on samples as homogeneous as possible, that is, containing either a large majority of reversibly porated cells, or a large majority of irreversibly porated ones. Due to the typical nonhomogeneity of electroporation in cells exposed to the electric field in large batches, homogeneous samples must be obtained by some method of cell separation. The most accurate separation devices are fluorescence- or magnetic-activated cell sorters (FACS and MACS), but they require labeling of cells by fluorescent or magnetic markers; moreover, they are large and expensive. In contrast, methods of DEP separation do not require labeling, and the devices are much smaller and relatively inexpensive to fabricate. Provided that the electric properties of irreversibly electroporated, reversibly electroporated, and nonelectroporated cells differ sufficiently, DEP methods could thus be used for simple and marker-free separation of these three classes.

Several different designs of DEP separation devices have been developed [10–12], with the inhomogeneity of the electric field generating the DEP force achieved either by the shapes of the electrodes [13, 14], or by inclusion of insulating structures into the otherwise largely homogeneous field [15, 16]. Some of these devices are based on opposite directions of the DEP force acting on different classes of cells [14, 17], and others on different magnitudes of this force [14, 17, 18]. A particularly useful subgroup of the latter devices is that based on DEP-field-flow fractionation (DEP-FFF) performed in a shallow flow-through microfluidic channel with electrodes at the bottom [19, 20]. The DEP-FFF devices are less sensitive to the variability of cell size and shape, allowing for successful separation of cells with smaller differences in their electric properties [21].

In DEP-FFF devices, the vertical position of each cell in the channel is determined by the equilibrium between the sedimentation force (sum of gravity and buoyancy) pulling the cells downwards, and the negative-DEP force generated by the electrodes at the bottom of the channel and pushing the cells upwards. Differences in electric properties of the cells affect the DEP force acting on them, but not the sedimentation force, leading to differences in the vertical equilibrium positions for the cells of the same type with differing electric properties (e.g., due to differences in their viability, phase of the cell cycle, stage of differentiation, or damage to the plasma membrane). In a shallow microfluidic channel, the flow is laminar and has a parabolic velocity profile, due to which the cells at different vertical positions have different velocities, with the cells at the vertical middle of the channel flowing the fastest, and those close to the bottom flowing the slowest [20, 22, 23]. By injecting a batch of cell suspension into the chamber and pumping it through the channel at a constant rate (the process henceforth referred to as *elution*), the cells closer to the vertical middle of the channel reach its output first, and those at lower positions follow later. Separation of two (or fractionation of several) classes of cells is then achieved by interchanging at appropriate times the containers into which the cells are collected at the output of the channel. For efficient DEP-FFF separation, it is important that at least one class of cells is subject to negative-DEP force (i.e., pushed upwards), as otherwise all the classes are pulled to the bottom of the channel and thus flow at the same velocity.

DEP-FFF systems are efficient in separation of various cell types [24], blood cells [25, 26], viable and non-viable cells [27], normal and cancerous cells [28], and different clones of cancerous cells [29]. As electroporation affects the electric properties of the cell, DEP could be particularly suitable for separation of electroporated cells from nonelectroporated ones. In our group, such separation has been attempted in a chamber with an array of castellated electrodes and opposite directions of the DEP force acting on porated and nonporated cells [30], with some spatial separation observed within the chamber, but with no feasible means of extracting the two classes of cells from the chamber separately. The inherent possibility of extraction of cells separated in DEP-FFF systems, together with their higher sensitivity, suggested to us that DEP-FFF is a promising approach for separation of electroporated and nonelectroporated cells.

A rough theoretical estimation of the feasibility of such separation can be performed by means of the Clausius–Mossotti theory, in which the dielectrophoretic force acting on a spherical cell enveloped by a single membrane (i.e., a single-shell model of a cell) in an electric field E is given by [31]:

$$\vec{F}_{\mathrm{DEP}} = 2\pi r^3 \varepsilon_e \,\mathrm{Re}\,(f_{\mathrm{CM}})\,\mathrm{grad}\,(E^2) \tag{1}$$

with f_{CM} the Clausius–Mossotti factor expressed as:

$$f_{\mathrm{CM}} = \frac{\varepsilon_c' - \varepsilon_e'}{\varepsilon_c' + 2\varepsilon_e'} \tag{2}$$

and with:

$$\varepsilon_{\mathrm{c}}' = \varepsilon_{\mathrm{m}}' \frac{\left(\frac{r}{r-d}\right)^3 + 2\frac{\varepsilon_{\mathrm{i}}' - \varepsilon_{\mathrm{m}}'}{\varepsilon_{\mathrm{i}}' + 2\varepsilon_{\mathrm{m}}'}}{\left(\frac{r}{r-d}\right)^3 - \frac{\varepsilon_{\mathrm{i}}' - \varepsilon_{\mathrm{m}}'}{\varepsilon_{\mathrm{i}}' + 2\varepsilon_{\mathrm{m}}'}} \tag{3}$$

where r is the cell radius, d is the membrane thickness, and $\varepsilon'_{\mathrm{e}}$, $\varepsilon'_{\mathrm{m}}$, and $\varepsilon'_{\mathrm{i}}$ are the complex dielectric permittivities of the external medium, membrane, and the cell interior (cytoplasm), respectively, each given by $\varepsilon' = \varepsilon - \mathrm{i}\sigma/(2\pi\nu)$, with ε and σ the dielectric permittivity and the electric conductivity of the region, and ν the frequency of the field.

Eqs. (1)–(3) show that at a given electric field, F_{DEP} is proportional to the real part of f_{CM}, which is a function of the field frequency ν that will henceforth be referred to as the DEP spectrum. Thus, fractionation by means of DEP-FFF of cells belonging to two classes with differences in electric properties is feasible if these differences result in the two classes having sufficiently different DEP spectra.

The aqueous pores formed in the lipid bilayer of the cell plasma membrane by electroporation increase the electric conductivity of the membrane (σ_{m}) and hence its permeability for ions. In low-conductivity media used for

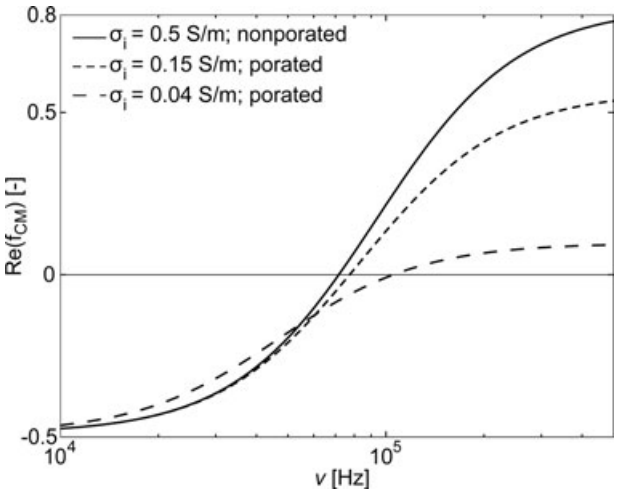

Figure 1. The theoretical estimates of the DEP spectra for nonporated (solid) and electroporated (dashed) CHO cells, with parameter values given in Table 1.

Table 1. The parameter values used for theoretical estimation of the DEP spectrum for nonporated CHO cells in the external medium as described in Section 2.1 and illustrated in Fig. 1; $\varepsilon_0 \approx 8.8542 \times 10^{-9}$ F/m

	Unit	Value	Source
r	m	5.9×10^{-6}	Measured
d	m	4.0×10^{-9}	[38]
σ_e	S/m	0.03	Measured
ε_e	F/m	$78 \times \varepsilon_0$	[39]
σ_m	S/m	3.0×10^{-7}	[40]
ε_m	F/m	$7 \times \varepsilon_0$	[41]
σ_i	S/m	0.50	[42]
ε_i	F/m	$60 \times \varepsilon_0$	[41]

DEP-FFF, this leads to a net outflow of ions that lowers the conductivity of the cell interior (σ_i). Electroporated cells are therefore generally characterized by a higher σ_m, and in low-conductivity media also by a lower σ_i with respect to nonporated cells. However, in reversibly electroporated cells both these effects are only temporary. Thus, after the initial increase of σ_m by several orders of magnitude [32,33], the membrane starts to recover within milliseconds and σ_m returns to its initial state within seconds [34–36], while the membrane ion pumps in nonexcitable cells take minutes to establish the initial ionic concentrations and thereby the initial value of σ_i [37] (this is the case even in a physiological-conductivity medium, while in low-conductivity media this process is even slower). Since DEP-FFF proceeds on the time scale of minutes, the initial increase of σ_m is too short-lived for utilization in fractionation of electroporated cells, while the decrease of σ_i may be sufficiently persistent for this purpose.

Figure 1 shows estimates of the DEP spectrum (the real part of f_{CM} as a function of electric field frequency), as defined by Eqs. (2) and (3), for nonporated and electroporated CHO cells, with all the parameter values for nonporated cells given in Table 1, and with two different scenarios for electroporated cells, with σ_i lowered from 0.5 to 0.15 and 0.04 S/m, respectively. Based on these estimates, the crossover frequency of the DEP spectrum for nonporated cells should be in the vicinity of 70 kHz, and electroporation should result in its shift toward higher frequencies; for efficient DEP-FFF fractionation; this estimate suggests that DEP-FFF should be efficient at frequencies up to 70 kHz, as this should make at least one class of cells subject to negative DEP. Here, we should note that electroporated cells differ from the idealized assumptions used here in at least four aspects (listed roughly in the order of decreasing importance): (i) σ_m and σ_i vary with time, (ii) σ_m also varies with position, as electroporation is the most intense in the membrane regions facing the electrodes used to deliver the electric field pulses, (iii) σ_m is moreover anisotropic, as the pores are perpendicular to the membrane, and (iv) electroporation-mediated transport across the membrane could also cause the value of ε_i to increase toward that of ε_e. Still, at least qualitatively, the prediction that electroporation results in an increase of the crossover frequency should hold, and this suggests that fractionation of irreversibly electroporated, reversibly electroporated, and nonelectroporated cells could be feasible.

In this paper, we describe the development and testing of a setup in which the DEP-FFF method described above is applicable for fractionation of electroporated cells. During the development phase, we used moderately heat-treated cells as a uniform and stable model of electroporated cells, optimizing the channel and electrode dimensions, flow rate, and electric field parameters for their efficient DEP-FFF separation from untreated cells. During the testing phase that followed, we used cells exposed to pulses of five different amplitudes rendering various fractions of nonporated, reversibly porated, and irreversibly porated cells, and performed the separation/fractionation at six different frequencies. We show that using such a system, DEP-FFF fractionation of irreversibly electroporated, reversibly electroporated, and nonelectroporated cells is feasible, and while it generally cannot yield completely pure samples, it is useful for their substantial refinement.

2 Materials and methods

2.1 Cells

CHO cells (European Collection of Cell Cultures, Salisbury, UK) were grown in the culture medium consisting of Ham's F-12 medium (PAA Laboratories, Pasching, Austria) supplemented with 2 mM glutamine (Sigma-Aldrich, St. Louis, MO, USA), 10% fetal bovine serum (PAA Laboratories) and antibiotics crystacillin (Pliva, Zagreb, Croatia) and gentamycin (Sigma-Aldrich), at 37°C in a humidified 5% CO_2 atmosphere.

Cells were detached from the flask surface by trypsination in 0.25% trypsin/EDTA (Sigma-Aldrich). The obtained suspension was centrifuged for 5 min (1000 rpm at 4°C) and resuspended in the DEP buffer consisting of iso-osmotic PBS [43] diluted with 250 mM sucrose to adjust the electric

conductivity to 27 mS/m at preserved iso-osmolarity. The suspension was again centrifuged and resuspended in the DEP buffer at final concentration of 2×10^7 cells/mL.

2.2 Heat treatment and electroporation

Heat-treated cells were obtained by placing the vial with the cells suspended in the culture medium (see Section 2.1) into a water bath at 50°C for 15 min before two centrifugations. This yielded cells retaining their normal size, shape, and appearance (as observable under a microscope), but with an increased electric conductivity of the membrane [44] and with no long-term viability [23]. On yeast and bacterial cells, heat-treatment is often performed at temperatures over 80°C [13,45], but with CHO cells such intense heating, while surely causing a larger effect on the membrane conductivity, would also result in excessive damage to the cells or even their complete disintegration.

Cell suspended in the DEP buffer (see Section 2.1) were electroporated in cuvettes with 1-mm distance between the electrodes (Eppendorf, Hamburg, Germany) by Cliniporator® (Igea, Carpi, Italy). A train of eight pulses with 100-μs duration and 1-Hz repetition frequency was delivered to the cuvette, with the pulse amplitude (electric field strength estimated as the ratio between the voltage delivered to the plate electrodes and the distance between them) of 1200, 1600, 2000, 2400, or 2800 V/cm. Within 5–10 s after the exposure to electroporative pulses, the cells were injected into the channel of the DEP-FFF chamber, and fractionation was initiated.

Fraction of electroporated cells was evaluated by assessing their permeability to propidium iodide (PI, Sigma-Aldrich), which cannot permeate an intact membrane, but fluoresces inside a cell. Immediately before exposure to electroporative pulses, PI was added to the cell suspension in final concentration of 100 μM. After the exposure, the fraction of cells displaying PI fluorescence was determined by counting the cells under a fluorescence microscope (Axiovert 200, Carl Zeiss MicroImaging, Jena, Germany) with a cooled CCD video camera (VisiCam 1280, Visitron Systems, Munich, Germany) and MetaMorph 7.0 image acquisition software (Molecular Devices, Sunnyvale, CA, USA). For each set of parameter values, at least 300 cells were counted, and each such experiment was repeated three times.

Fraction of viable cells was assessed by placing 5000 cells per well on a 96-well microtiter plate (TPP, Trasadingen, Switzerland) after pulsation. Culture medium was added to bring the total volume in each well to 100 μL. After 48 h of incubation, the cell viability test was performed using the MTS assay (Cell Titer 96® Aqueous One Solution Cell Proliferation Assay, Promega, Madison, WI, USA). Fluorescence intensity was measured with a spectrofluorometer (Tecan Infinite M200, Tecan, Grödig, Austria), and the viability was calculated as the ratio of fluorescence intensities of cells exposed to an electroporating field and those unexposed (100% viable). Each experiment was repeated three times, with six wells per set of parameter values in each repetition.

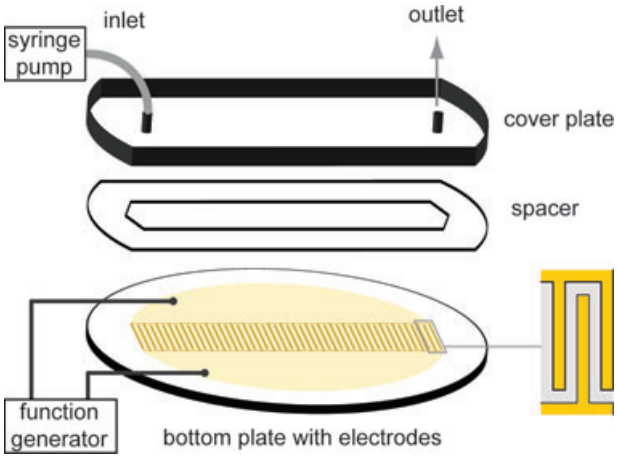

Figure 2. Schematic drawing of the DEP-FFF chamber.

2.3 DEP-FFF chamber

The DEP-FFF chamber was designed and fabricated as described in detail in Čemažar et al. [23], and is shown in the schematic drawing in Fig. 2. Pyrex glass (Pyrex 7740, Corning Inc., Corning, NY, USA) with 100-mm diameter and 0.7-mm thickness was used as a basis for the electrodes, onto which a 50-nm layer of chromium and a 150-nm layer of gold were deposited by sputtering. The electrodes 76-mm long, 20-mm wide, and consisting of 400 interdigitated bars 115-μm wide with 75-μm interelectrode gaps, were fabricated by photolithography and subsequent wet etching and cleaning.

The top of the chamber was made of soda-lime glass, with holes for inlet and outlet drilled through. Double-sided self-adhesive tape (Isotrade Jereb, Ljubljana, Slovenia) 100-μm thick with an opening cut into it was used as a spacer between the two glass surfaces, forming a channel 8-cm long, 2-cm wide, and 100-μm high. The nontoxic water-resistant acrylic glue of the tape loses its adhesive properties at temperatures above 70°C and allows for easy disassembly, cleaning, and reassembly of the chamber.

2.4 Fractionation

For DEP-FFF fractionation, a voltage of 3 V peak-to-peak amplitude (±1.5 V) at 35, 50, 65, 80, 95, or 110 kHz frequency (chosen as to cover the interval containing the expected crossover frequencies for all investigated cell groups) was delivered to the electrodes of the chamber by a voltage function generator (33250A, Agilent Technologies, Santa Clara, CA, USA). Silicon tubes with 1.5-mm inside diameter were connected to the chamber, and a 1-mL syringe was mounted onto a syringe pump (Aladdin, WPI, Boulevard Sarasota, FL, USA). The chamber was prefilled with the DEP buffer (see Section 2.1), and then the cells suspended in the DEP buffer (total suspension volume of 5 μL) were injected into the channel and pumped through it at a constant flow rate (either at 30 or 60 μL/min, which corresponds to the average flow

velocity of 0.35 and 0.70 mm/s, respectively). The flow of cell suspension through the channel was monitored under the microscope (Axiovert 200, Carl Zeiss MicroImaging). A sequence of images was taken at the output, one image every 2 s, and the number of cells in each image was divided by the number of cells in all the images of the sequence to obtain an estimate of the fraction of cells reaching the chamber output as a function of time (the *elution profile*). Every measurement was repeated three times.

3 Results and discussion

3.1 Development of the DEP-FFF separation method

Our DEP-FFF chamber was first developed and optimized for efficient separation of moderately heat-treated CHO cells (50°C for 15 min) from untreated ones [23]. The dimensions as given in Section 2.3 were optimized based on numerical computations of the electric field, its gradient, and the field-flow velocity profile.

Heat treatment increases the fluidity of the lipid bilayer and denatures the transport proteins (pumps and channels) in the cell plasma membrane. This results in an increased electric conductivity of the membrane [44] and hence its permeability for ions, but with the 50°C, 15-min treatment applied here, the cells still retained their normal size, shape, and appearance (as observable under a microscope). In a low-conductivity medium used for DEP-FFF, this leads to a net outflow of ions that lowers the conductivity of the cell interior. Therefore, the effect of heat treatment on the electric properties of the cells should at least qualitatively be similar to the effect of electroporation as outlined in Section 1. During the chamber development phase, we have thus used the 50°C heat-treated cells as a rough approximation of electroporated cells characterized by its uniformity and stability. Namely, the heat-induced changes of the electric properties of the cell are largely irreversible, while changes caused by electroporation can also be reversible, with the membrane returning to the initial state within seconds [34–36], and the membrane pumps establishing the physiological ionic concentrations in the cell interior within minutes [37]. As a consequence, with respect to the changes in electric properties, the samples of electroporated cells are generally both more heterogeneous and more time-varying than samples of heat-treated cells.

Separation protocol was optimized by eluting batches of 10^5 cells at various frequencies and peak-to-peak amplitudes of the voltage generating the negative-DEP force, and at various flow rates. Optimal separation of heat-treated and -untreated CHO cells was obtained with a 6 V peak-to-peak voltage (±3 V) at 65 kHz, with a 5 μL batch of the cell suspension eluted at a 30 μL/min flow rate (average flow velocity of 0.35 mm/s), at which the separation process was completed in under 14 min. Our measurements show that the 65 kHz frequency is still in the range of negative DEP for both cell groups, but that it is closer to the crossover frequency for untreated than for heat-treated CHO cells, which

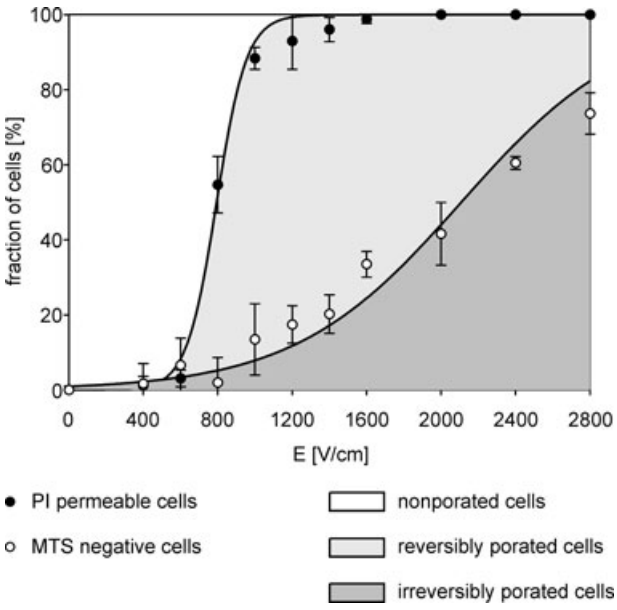

Figure 3. Fractions of electroporated (PI permeable) and nonviable (MTS negative) CHO cells. The difference between the two fractions represents the fraction of reversibly electroporated cells (light gray area).

is in agreement with the theoretical expectations outlined above (see also e.g., Fig. 8 in [23]). Due to this, the DEP force is pushing both groups of cells upwards, but the force acting on heat-treated cells is larger, so that they have a higher vertical equilibrium position, hence a higher flow rate, and they reach the output faster (based on Eq. (2) from [25], estimated average levitation heights were 11 and 7 μm for heat-treated and untreated cells, respectively). The best separation results were achieved by collecting the eluted cells at the chamber output between the 5th and the 7th min and between the 11th and the 13th min after the start of the flow, yielding 93% of heat-treated cells and 77% of untreated cells, respectively.

3.2 Cell electroporation and viability as functions of pulse amplitude

Figure 3 shows the fractions of electroporated and nonviable (i.e., irreversibly electroporated) cells as functions of pulse amplitude used for electroporation (expressed as the ratio of the voltage applied to the electrodes and the distance between them). The cells exposed to 1200 V/cm pulses (containing ∼77% of reversibly porated cells) and 2800 V/cm pulses (containing ∼74% of irreversibly porated cells) were deemed the most representative samples of reversibly and irreversibly electroporated cells, respectively. Namely, pulse amplitudes exceeding 2800 V/cm led to considerable fractions of disintegrated cells, resulting in substantial release of intracellular contents and debris, which could affect the properties of the DEP buffer and the separation/fractionation process.

3.3 Fractionation of samples exposed to different pulse amplitudes

To test the ability of our chamber to fractionate irreversibly porated, reversibly porated, and nonporated cells, we first applied the protocol optimized with heat-treated cells (see Section 3.1), with 65 kHz frequency, but with the voltage generating the DEP field reduced to 3 V peak-to-peak (±1.5 V). This reduced the electric field in the chamber by one-half, and thereby the DEP force by three quarters (see Eq. (1)), but with the maximal electric field reduced from 400 to 200 V/cm, it completely eliminated the possibility of the cells being electroporated by the DEP field itself. Namely, with the 75-μm interelectrode gap, even the 6 V peak-to-peak voltage (±3 V) applied in the separation of heat-treated and -untreated cells resulted in the maximal electric field of 400 V/cm, which according to Fig. 3 does not yield any statistically significant level of electroporation, but at the maximal field of 200 V/cm generated with 3 V (±1.5 V), absence of electroporation can be taken for certain. In addition, to decrease the effects of recovery of reversibly porated cells that renders them increasingly similar to nonporated cells, the flow rate through the channel was increased to 60 μL/min, double the rate used for separation of heat-treated and -untreated cells. Thus, the fractionation process was completed in less than 7 min. We then repeated these experiments also at 35, 50, 80, 95, and 110 kHz frequencies, focusing on the effect of the frequency-dependent changes of f_{CM}, and thus of the DEP force, exerted on the elution profiles of different cell groups.

Figure 4A–C shows the elution profile of cells exposed to 0, 1200, 1600, 2000, 2400, and 2800 V/cm and then eluted at 35, 65, and 95 kHz. Roughly in line with the theoretical predictions as given by Fig. 1, at 35 kHz the peaks of the profiles are very close together, while at 65 and 95 kHz the electroporated cells on the average reach the output faster, reflecting their higher vertical equilibrium positions due to the more negative (or at least less-positive) DEP force. Still, according to Fig. 1, the negative-DEP force acting on the cells at 35 kHz should be considerably stronger–and the cells should reach the output much faster–than at 65 or 95 kHz, while the results in Fig. 4 show that this effect is present in nonporated and reversibly porated cells, but barely detectable in irreversibly porated cells. This implies that for a more accurate agreement between theory and experiments, the temporal and spatial variability of the conductivities characteristic of electroporation, and perhaps also the anisotropy of the membrane conductivity, would likely have to be taken into account.

At 65 kHz, the peaks of the profiles are the most distinctive, and the irreversibly porated cells could be efficiently separated from the nonporated and reversibly porated cells treated as a single class; collecting the cells at the chamber output between the 60th and the 100th s, and between the 240th and the 360th s after the start of the flow, yielded 88% of irreversibly porated cells, and 99% of nonporated and reversibly porated cells counted together, respectively. The elution profiles of the nonporated and reversibly porated cells are

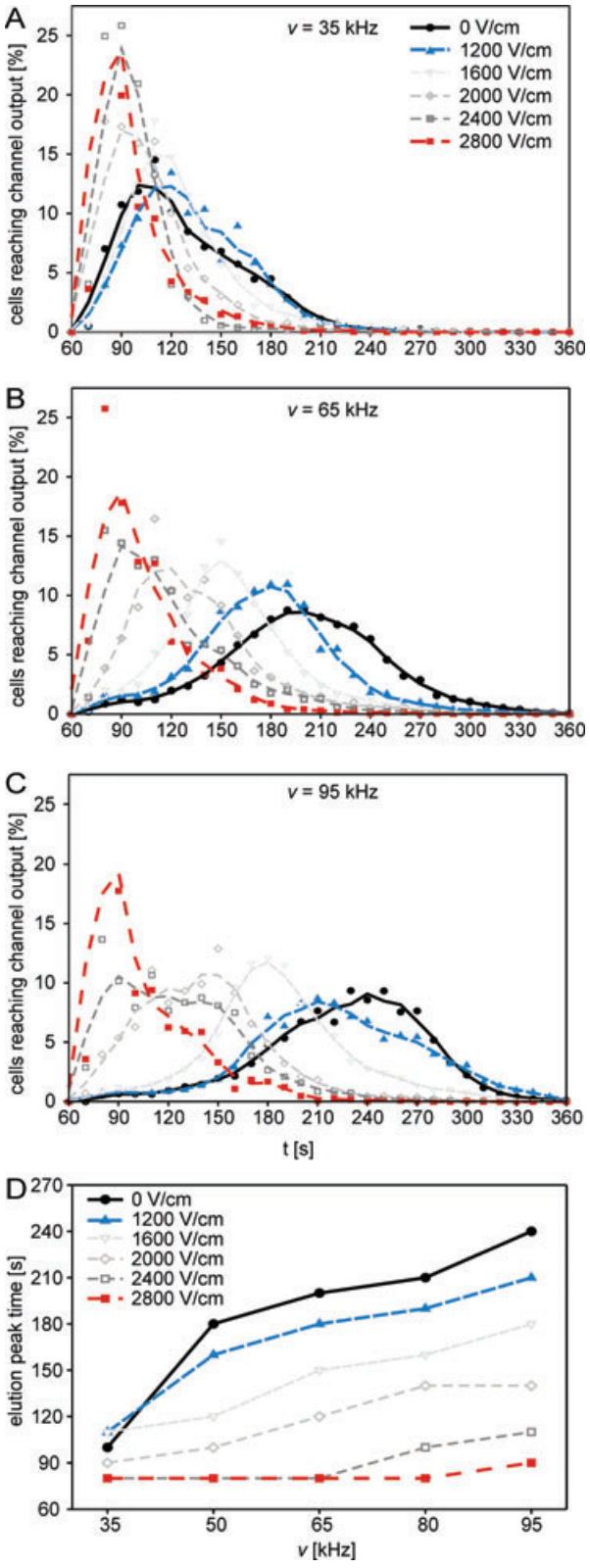

Figure 4. (A–C) Elution profiles of CHO cells exposed to electroporative pulses of various amplitudes, and subsequently DEP-FFF fractionated at 35, 65, and 95 kHz. (D) Elution peak times for these cells as functions of DEP-FFF frequency. All the data points are averages of three independent measurements.

too close together to allow for a similarly high efficiency of separation of these two classes of cells, largely due to the fact that the recovery of the reversibly porated cells toward their pre-poration state is faster than their passage through the separation channel. Still, as can be seen in Fig. 4A–C, substantial refinement is achievable also for these two classes.

The three parameters that could in principle be varied to improve the fractionation efficiency were the flow rate, and the peak-to-peak amplitude and frequency of the voltage generating the DEP force. While a further increase of the flow rate was feasible, and with faster elution the reversibly porated cells would recover to a smaller extent during the fractionation, we found that this gain is largely neutralized by the squeezing of the elution profiles as a whole along the time axis, which also brings their peaks closer together. An increase of the voltage delivered to the electrodes for DEP-FFF fractionation would increase the negative-DEP force acting on each of the cell classes correspondingly, amplifying also the differences in elution profiles, but as discussed above, we chose to avoid it as to ensure that no unintentional electroporation is caused by the electric field used to generate the DEP force.

Thus, we investigated systematically the influence of the frequency of the voltage generating the DEP force, focusing particularly on the frequency ranges where DEP is negative and thus favorable for efficient DEP-FFF. Figure 4D shows the times at which the peaks of the individual elution profiles (the elution peaks) occurred for cells previously exposed to pulses with amplitudes from 0 to 2800 V/cm as functions of DEP-FFF frequencies from 35 to 95 kHz. The decrease of the DEP-FFF frequency below 65 kHz resulted in gradual convergence of the elution peaks of nonporated, reversibly porated, and irreversibly porated cells, and at 35 kHz the fractionation effects were already radically reduced. Still, at 50 kHz, despite the closer peaks compared to 65 kHz, there was slightly less overlapping of the complete profiles of the groups exposed to 0, 1200, and 2800 V/cm, yielding the best achievable fractionation of nonporated, reversibly porated, and irreversibly porated cells as three separate classes. Namely, already by collecting the cells at the chamber output in three contiguous time intervals–between the 60th and the 150th s, between the 150th and the 180th s, and between the 180th and 360th s after the start of the flow–we obtained 62% of irreversibly porated cells, 56% of reversibly porated cells, and 64% of nonporated cells, respectively. With noncontiguous time intervals, the efficiency of fractionation was improved further for irreversibly porated cells (reaching 87% for the interval between the 60th and the 100th s) and for nonporated cells (reaching 80% for the interval between the 240th and the 300th s). Thus, fractionation of irreversibly electroporated, reversibly electroporated, and nonelectroporated cells by DEP-FFF is feasible, and while it did not yield highly purified samples (e.g., efficiencies of 90% or higher), it can be used for their substantial refinement, which can be useful for in vitro investigations of various effects of reversible or/and irreversible poration.

Figure 4D also shows that an increase of the DEP-FFF frequency from 65 to 80 kHz resulted in an increased shift between the elution peak of the irreversibly porated cells on one side, and the elution peaks of the nonporated and reversibly porated cells on the other. Collecting the cells at the chamber output between the 60th and the 100th s, and between the 240th and the 360th s, yielded 92% of irreversibly porated cells, and 99% of nonporated and reversibly porated cells counted together, respectively—a somewhat better separation efficiency than at 65 kHz. However, a further increase in DEP-FFF frequency led to pronounced slowdowns of the profiles, implying the undesired transition from negative into positive DEP (see Fig. 1), where the cells are pulled toward the electrodes, and start to roll at (or close to) the bottom of the chamber, instead of freely floating.

It is worth noting that the separation and fractionation efficiencies stated above were obtained proceeding from a sample containing equal fractions of nonporated, reversibly porated, and irreversibly porated cells; more precisely, these efficiencies follow from the elution profiles, as given in Fig. 4, for a suspension formed from equal amounts of cells exposed to 0, 1200, and 2800 V/cm pulses. In realistic situations, the amplitude of the pulses to which the cells are exposed in order to achieve electroporation already leads to a sample with a higher content of one class with respect to the other two (e.g., close to 100% nonporated cells at amplitudes below 600 V/cm, over 80% of reversibly porated cells at 1200 V/cm, and about 70% of irreversibly porate cells at 2800 V/cm, see Fig. 3). As a consequence, by performing a suitable DEP-FFF separation or fractionation of cells exposed to a particular amplitude of electroporative pulses, the final yield of a particular class of cells will be much higher than the yields obtained with equal initial fractions of the three classes. For example, by exposing the cells to 1600 V/cm pulses, the sample will contain practically no nonporated cells (see Fig. 3), hence the DEP-FFF fractionation will in fact amount to separation of reversibly porated from irreversibly porated cells.

In our setup, the cells were electroporated in cuvettes standardly used for this purpose, and then transferred into the DEP-FFF chamber for fractionation. However, electroporation can also be performed in microfluidic devices [46–48]. A merger of microfluidic designs for electroporation and fractionation into a single device would eliminate the need for intermediary transfer of cells, shortening the delay between electroporation and the start of fractionation.

4 Concluding remarks

Our results obtained with CHO cells indicate that with a suitably designed chamber and a sufficiently optimized protocol, DEP-FFF can be used both for separation of irreversibly electroporated cells from nonelectroporated and reversibly electroporated ones considered as a single class (with high efficiency), and for fractionation of irreversibly porated, reversibly porated, and nonporated cells as three separate classes (with moderate efficiency). The general dimensions of the chamber used here (roughly 100-μm electrode width, interelectrode gap, and channel height, and 6–10 cm channel

length) should be adequate irrespective of the specific cells to be separated or fractionated after electroporation. On the other hand, the protocol parameters—in our case 60 μL/min flow rate (average flow velocity of 0.7 mm/s), 3 V peak-to-peak voltage between the electrodes, 50/65/80 kHz frequency—are likely to be optimizable further for each particular type of cells, experimental conditions under which they are electroporated, and composition of the DEP buffer.

This research was supported by the Slovenian Research Agency (Research Program P2–0249) and conducted in the scope of the EBAM European Associated Laboratory (LEA).

The authors have declared no conflicts of interest.

5 References

[1] Neumann, E., Rosenheck, K., *J. Membrane Biol.* 1972, *10*, 279–290.

[2] Weaver, J., Chizmadzhev, Y., *Bioelectrochem. Bioenerg.* 1996, *41*, 135–160.

[3] Weaver, J. C., *IEEE Trans. Dielect. Electr. Insul.* 2003, *10*, 754– 768.

[4] Sersa, G., Miklavcic, D., Cemazar, M., Rudolf, Z., Pucihar, G., Snoj, M., *Eur. J. Surg. Oncol.* 2008, *34*, 232–240.

[5] André, F., Mir, L. M., *Gene Ther.* 2004, *11*(Suppl 1), S33–S42.

[6] Lee, E. W., Thai, S., Kee, S. T., *Gut Liver* 2010, *4*(Suppl 1), S99–S104.

[7] Sack, M., Sigler, J., Frenzel, S., Eing, C., Arnold, J., Michelberger, T., Frey, W., Attmann, F., Stukenbrock, L., Müller, G., *Food Eng. Rev.* 2010, *2*, 147–156.

[8] Morales-de la Peña, M., Elez-Martínez, P., Martín-Belloso, O., *Food Eng. Rev.* 2011, *3*, 94–107.

[9] Puc, M., Kotnik, T., Mir, L. M., Miklavcic, D., *Bioelectrochemistry* 2003, *60*, 1–10.

[10] Pethig, R., *Biomicrofluidics* 2010, *4*, 022811.

[11] Çetin, B., Li, D., *Electrophoresis* 2011, *32*, 2410–2427.

[12] Gagnon, Z. R., *Electrophoresis* 2011, *32*, 2466–2487.

[13] Li, H. B., Bashir, R., *Sens. Actuators B Chem.* 2002, *86*, 215–221.

[14] Khoshmanesh, K., Nahavandi, S., Baratchi, S., Mitchell, A., Kalantar-zadeh, K., *Biosens. Bioelectron.* 2011, *26*, 1800–1814.

[15] Lapizco-Encinas, B. H., Simmons, B. A., Cummings, E. B., Fintschenko, Y., *Anal. Chem.* 2004, *76*, 1571–1579.

[16] Kang, Y., Cetin, B., Wu, Z., Li, D., *Electrochim. Acta* 2009, *54*, 1715–1720.

[17] Pamme, N., *Lab Chip* 2007, *7*, 1644–1659.

[18] Roda, B., Zattoni, A., Reschiglian, P., Moon, M. H., Mirasoli, M., Michelini, E., Roda, A., *Anal. Chim. Acta* 2009, *635*, 132–143.

[19] Huang, Y., Wang, X. B., Becker, F. F., Gascoyne, P. R. C., *Biophys. J.* 1997, *73*, 1118–1129.

[20] Markx, G. H., Rousselet, J., Pethig, R., *J. Liq. Chromatogr. Related Technol.* 1997, *20*, 2857–2872.

[21] Pratt, E. D., Huang, C., Hawkins, B. G., Gleghorn, J. P., Kirby, B. J., *Chem. Eng. Sci.* 2011, *66*, 1508–1522.

[22] Giddings, J., *Science* 1993, *260*, 1456–1465.

[23] Cemazar, J., Vrtacnik, D., Amon, S., Kotnik, T., *IEEE Trans. Nanobiosci.* 2011, *10*, 36–43.

[24] Gasperis, G. D., Yang, J., Becker, F. F., Gascoyne, P. R. C., Wang, X.-B., *Biomed. Microdevices* 1999, *2*, 41–49.

[25] Wang, X.-B., Yang, J., Huang, Y., Vykoukal, J., Becker, F. F., Gascoyne, P. R. C., *Anal. Chem.* 2000, *72*, 832–839.

[26] Holmes, D., Green, N. G., Morgan, H., *IEEE Eng. Med. Biol. Mag.* 2003, *22*, 85–90.

[27] Yu, L. M., Iliescu, C., Xu, G. L., Tay, F. E. H., *J. Microelectromech. Syst.* 2007, *16*, 1120–1129.

[28] Yang, J., Huang, Y., Wang, X. B., Becker, F. F., Gascoyne, P. R. C., *Anal. Chem.* 1999, *71*, 911–918.

[29] Sabuncu, A. C., Liu, J. A., Beebe, S. J., Beskok, A., *Biomicrofluidics* 2010, *4*, 021101.

[30] Oblak, J., Križaj, D., Amon, S., Maček-Lebar, A., Miklavčič, D., *Bioelectrochemistry* 2007, *71*, 164–171.

[31] Jones, T. B., *IEEE Eng. Med. Biol. Mag.* 2003, *22*, 33–42.

[32] Kinosita Jr., K., Tsong, T. Y., *Biochim. Biophys. Acta Biomembr.* 1979, *554*, 479–497.

[33] Benz, R., Conti, F., *Biochim. Biophys. Acta Biomembr.* 1981, *645*, 115–123.

[34] Hibino, M., Itoh, H., Kinosita, K., *Biophys. J.* 1993, *64*, 1789–1800.

[35] Schmeer, M., Seipp, T., Pliquett, U., Kakorin, S., Neumann, E., *Phys. Chem. Chem. Phys.* 2004, *6*, 5564–5574.

[36] Pucihar, G., Kotnik, T., Miklavcic, D., Teissie, J., *Biophys. J.* 2008, *95*, 2837–2848.

[37] Ando, J., Smith, N. I., Fujita, K., Kawata, S., *Eur. Biophys. J.* 2009, *38*, 255–262.

[38] Alberts, B., Johnson, A., Lewis, J., Raff, M., Roberts, K., Walter, P., *Molecular Biology of the Cell*, Fourth Edition, Garland Science, New York 2002.

[39] Buchner, R., Hefter, G. T., May, P. M., *J. Phys. Chem. A* 1999, *103*, 1–9.

[40] Gascoyne, P. R. C., Pethig, R., Burt, J. P. H., Becker, F. F., *Biochim. Biophys. Acta* 1993, *1149*, 119–126.

[41] Hu, Q., Joshi, R. P., Beskok, A., *J. Appl. Phys.* 2009, *106*, 024701.

[42] Holzel, R., Lamprecht, I., *Biochim. Biophys. Acta* 1992, *1104*, 195–200.

[43] Ušaj, M., Trontelj, K., Hudej, R., Kandušer, M., Miklavčič, D., *Radiol. Oncol.* 2009, *43*, 108–119.

[44] Huang, Y., Hölzel, R., Pethig, R., Wang, X. B., *Phys. Med. Biol.* 1992, *37*, 1499–1517.

[45] Iliescu, C., Yu, L. M., Tay, F. E. H., Chen, B. T., *Sens. Actuators B Chem.* 2008, *129*, 491–496.

[46] Huang, Y., Rubinsky, B., *Sens. Actuators A Phys.* 2003, *104*, 205–212.

[47] Lu, H., Schmidt, M. A., Jensen, K. F., *Lab Chip* 2005, *5*, 23–29.

[48] Khine, M., Lau, A., Ionescu-Zanetti, C., Seo, J., Lee, L. P., *Lab Chip* 2005, *5*, 38–43.

